NATIONAL ADVISORY COMMITTEE FOR AERONAUTICS

TECHNICAL NOTE 3474

RAPID RADIANT-HEATING TESTS OF MULTIWEB BEAMS

By Joseph N. Kotanchik, Aldie E. Johnson, Jr.,
and Robert D. Ross

Langley Aeronautical Laboratory
Langley Field, Va.

Washington
September 1955

NATIONAL ADVISORY COMMITTEE FOR AERONAUTI

TECHNICAL NOTE 3474

RAPID RADIANT-HEATING TESTS OF MULTIWEB BEAMS

By Joseph N. Kotanchik, Aldie E. Johnson, Jr.,
and Robert D. Ross

SUMMARY

Four multiweb box beams were subjected to radiant heating at rates up to 90 Btu/ft^2-sec. The heating was unsymmetrical (only one cover of each beam was heated) and no external loading was applied during heating. Measured temperatures in the covers and webs are given. Thermal stresses buckled the covers while the beams were being heated and the webs as the beams were cooling. The temperatures at which buckling of the covers occurred were approximately the same for beams with ribs as for beams without ribs. Measured strains in the webs were used to determine bending distortions and stresses. Stresses at buckling were found to agree with those predicted by an elementary thermal-stress analysis. A description of the rapid-heating apparatus is presented.

INTRODUCTION

The high-temperature boundary layer in supersonic flight or thermal radiation of thermonuclear explosions may subject future aircraft to very high heating rates. Such rapid heating of the surface of the aircraft can induce thermal stresses in the load-carrying structure which may have serious consequences aerodynamically as well as structurally. For example, thermal stresses can attain magnitudes sufficient to buckle the skin and thus destroy the aerodynamic smoothness of the surface or they may decrease the stiffness of the structure and make it more susceptible to aeroelastic difficulties.

The purpose of the present investigation was to observe the effects of rapid heating on a shell type of structure. Multiweb box beams were subjected to high rates of heating by exposing one cover of each beam to a radiant-heat source. No external loading was applied to the beams during heating. Temperatures in the heated skin and in the webs, distortions of the skin, and strains in the webs were measured during the heating cycle.

The heating rates and the sizes of heated areas of the specimens of the present investigation required a combination of density of energy and total energy which necessitated the development of special heat-radiating apparatus. This apparatus is described in appendix A.

SPECIMENS, TESTS, AND INSTRUMENTATION

Four multiweb box beams, two with ribs (as shown in fig. 1) and two without ribs, were subjected to rapid heating. The material of the beams was clad 2024-T4 (formerly clad 24S-T4) aluminum-alloy sheet. Figure 2 shows one of the box beams in testing position in front of the heat radiator.

Tests

Of the four beams subjected to rapid heating, two beams, one with ribs and one without ribs, were heated at a rate of about 80 Btu/ft^2-sec and the remaining two at about 25 Btu/ft^2-sec. Heat was applied to one cover only of each beam and no external loading was applied during the heating cycle. The durations of heating were about 4 seconds at the higher rate and 14 seconds at the lower rate. The data on times, temperatures, and heating rates are presented in table I. Heating of the specimens was by radiation. A detailed description of the radiator and of its performance is presented in appendix A.

Instrumentation

Beams with ribs.- Each beam contained 15 thermocouples on the heated cover and interior webs, 10 strain gages on 1 interior web, and 4 cantilever-type gages to detect buckling of the cover. The locations of the thermocouples and strain gages are shown in figure 3(a). Thermocouples were made from No. 30 iron-constantan wire with the junctions peened into a small hole and then welded to the beam. Strain gages were Baldwin type AB-5 SR-4 resistance wire gages. All data were recorded on two Miller oscillographs in synchronization.

Each cantilever gage consisted of an aluminum-alloy cantilever beam and a steel pin with conical ends; one end of the pin rested against the inner surface of the heated cover and the other end rested against the tip of the cantilever beam. The cantilevers may be seen in figure 2; they are attached to the unheated side of the beam and the steel pins pass through small holes in the unheated cover. Displacements of the cover out of its original plane produced deflection of the cantilever

beams, and the changes in strain at the root of the cantilever, measured by wire strain gages, served as an indication of buckling of the beam cover.

Beams without ribs.- Instrumentation of the beams without ribs consisted of 14 thermocouples on the covers and 1 interior web, 6 strain gages on the other interior web, and 4 cantilever gages. The locations of thermocouples and strain gages are shown in figure 3(b). All data were recorded on two Miller oscillographs in synchronization.

RESULTS AND DISCUSSION

Beam Behavior During Heating Cycle

A brief description of the typical behavior of a beam and the sequence of events during the heating cycle will aid the presentation of results. Upon exposure of the beam to the heat the cover temperature increased rapidly - approximately 200° F and 60° F per second for the high and low rates, respectively. The expansion of the cover produced curvature of the beam, with the convex side toward the heater. Longitudinal expansion of the cover, restrained by the cooler webs, resulted in induced compressive stresses in the cover and corresponding tensile stresses in the webs. These stresses increased in magnitude until the cover buckled.

At the conclusion of heating, the cover temperature was at its maximum, but a large part of each web had undergone no temperature change. At a relatively long time after heating ceased, the webs developed buckles near the hot cover. The times at which the webs buckled varied considerably inasmuch as the beams were cooled simply by blowing room air over them. When the entire beam was again at room temperature, deep permanent buckles remained in the heated cover and in the webs, and the beam was bent concave toward the heater.

Temperature Distributions

The measured temperature rise (from room temperature, approximately 80° F) in the covers and webs of the four beams is shown in figures 4 to 7 at times corresponding to three significant events of the heating cycle: buckling of the cover during heating (as determined by displacements of the cantilever gages), maximum cover temperature at conclusion of heating, and buckling of the webs during cooling of the beam. The temperature is shown as a function of distance from the center of the beam. When distances from the center of the beam to thermocouples in the cover were determined, the juncture of web and cover was taken at the center of the

rivet in the web attachment flange. It should be noted that, for figures 4 to 7, the temperature at the juncture of web and flange was measured by a thermocouple on the inside face of the web attachment flange; this temperature is therefore lower than some average temperature (which might be considered more representative) of the web-cover juncture.

Temperature distributions at time of buckling.- For both heating rates used in this investigation, the temperature-distribution curves show that, when the cover buckled, most of the webs had undergone no appreciable change in temperature and most of the cover was near the maximum cover temperature. Buckling of the covers for all the beams could therefore be expected at about the same temperature. The data (parts (a), figs. 4 to 7) show that buckling occurred when the temperature rise in the cover of each beam was approximately 500° F.

Temperature distributions at maximum cover temperatures.- The temperature distributions at maximum cover temperature are similar to those at buckling. Maximum cover-temperature rises were 700° F to 1,000° F approximately, but the center of the web and much of the web between the center and the heated cover had experienced little temperature rise.

Temperature distribution at time of buckling of webs.- Buckling of the webs occurred a relatively long time after heating had ceased and after most of the web had been heated to some extent by conduction from the hot cover. Temperature gradients were greatly decreased from those at buckling of the cover and at conclusion of heating.

Thermal Strains

Longitudinal strains were measured on the webs of the beams during the heating cycle. Analysis of these data showed that strain varied linearly across the depth of the beam and reached maximum values at a time which coincided with an indication of buckling displacements in the covers. The strain distribution at a time before buckling, at the buckling time, and at a time near maximum temperature is plotted as a function of beam depth in figure 8 for beams 1 and 2. Extrapolation of straight lines through the data yields values of strain in the covers and locates the position of the neutral axis as the beams bend during heating. The reversal in strains can be attributed to the abrupt change in stiffness of the heated cover when buckling occurs.

A typical strain-time history, obtained from a pair of back-to-back strain gages, is presented in figure 9 for the longitudinal strains at the center line of a web of beam 3. Tensile strain was induced in the web as the heating began, and the strain increased uniformly until the the cover buckled. After the cover buckled, strain in the web decreased; initially, the decrease was rather abrupt but became more gradual after

heating was discontinued. The web strains shown by the curves of figure 9 include thermal expansion for times after approximately 15 seconds; for those times the web material at the gage location was being heated by conduction from the hot cover. Divergence of the curves for the back-to-back gages in the range of 50 to 60 seconds indicates the inception of buckling of the web. The web-buckling times, however, were determined from strain reversal of one of the pairs of gages. Because of the manner in which the web was heated, web buckling was a progressive phenomenon and was not symmetrical with respect to the longitudinal center line of the web.

Thermal Stresses

From the value of cover strain for the time at which buckling occurred (determined from fig. 8 for the times of 2.3 and 8.4 seconds for beams 1 and 2, respectively), a cover stress at buckling can be determined from the equation

$$\sigma = E(\epsilon - \alpha \Delta T)$$

where

E	modulus of elasticity at temperature
ϵ	cover strain
α	coefficient of thermal expansion
ΔT	temperature rise in cover

The buckling stresses thus determined for the covers of beams 1 and 2 are 20,400 psi and 24,400 psi, respectively.

In appendix B, expressions are derived for the thermal stresses in an idealized multiweb beam with a temperature distribution as shown in figure 10 - one cover at a high temperature and the web and other cover at a low temperature. The stress in the heated cover is given by equation (B9) of appendix B. The actual temperature distributions in the beams (figs. 4 to 7) are represented approximately by the idealized distribution used in the derivation. The calculated thermal stress in the cover, when the heated cover is at 580° F and the remainder of the cross section is at 80° F, is 20,900 psi. These temperatures are approximately the temperatures measured in each test specimen at the time of buckling of the heated cover. This calculated stress level is in agreement with the stress indicated by the strain measurements and corresponds to a buckling-stress coefficient $k = 4.5$ for a width of cover plate equal to the distance between web lines. A value of k somewhat greater than 4 (corresponding to simple support at the web lines) appears to be reasonable.

Permanent Deformations

Figure 11 shows the deformations of a beam subjected to rapid heating. The cover of beam 3 before heating is shown in figure 11(a); the permanent buckles remaining in the cover after heating are shown in figure 11(b). A profile of the cover deformation taken longitudinally through the center of each bay is shown in figure 11(c). For this particular beam the cover was initially slightly curved as indicated by the deviation of the profile of the cover before heating, shown by the top heavy line, from the light, straight line through the ends of the beam. The profile after heating is shown by the bottom line and the shaded area indicates the amount of permanent deformation.

CONCLUSIONS

Temperature distributions were measured in the covers and webs of four multiweb box beams subjected to rapid heating at nominal rates of 25 and 80 Btu/ft^2-sec. Only one cover of each beam was heated and no external loading was applied. Similar results were obtained at both heating rates and for beams with and without ribs.

Compressive thermal stresses induced in the heated covers by the restraint of the unheated parts of the beams were sufficient to cause buckling. The thermal stresses calculated from the measured strains at buckling were in agreement with the stresses predicted by an elementary thermal-stress analysis. A reversal in bending distortion was noted at buckling which was attributed to a sudden loss in stiffness in the heated covers.

In addition to cover buckling, buckles developed in the webs as the beams cooled. Upon cooling to room temperature, the buckles remained in the beams and were superposed on a permanent bending distortion.

Langley Aeronautical Laboratory,
National Advisory Committee for Aeronautics,
Langley Field, Va., May 27, 1955.

APPENDIX A

RAPID-HEATING APPARATUS

The heat radiator used in the present tests was developed for the purpose of investigating transient heating effects in aircraft structures. Because heating rates of 30 Btu/ft^2-sec were attained in portions of the structures of research missiles, the requirement was made that the transient heating apparatus be capable of equal or higher heating rates. Heating rates of such magnitude are substantially higher than those that are provided by industrial installations employing radiant heating of relatively large areas.

Construction of Radiant Heater

The construction of the radiant heater is illustrated in figure 12. The heat-radiating element is a graphite rod heated to approximately 4,700° F by passing electric current through the rod. The rod is clamped at the ends in graphite blocks which serve as mechanical supports and as terminals through which the electrical current passes. Each basic heating unit, consisting of a graphite rod and terminal blocks, is bolted at the ends to nonconducting asbestos-cement sheets. A ceramic spacer is placed between the graphite terminal and the asbestos-cement sheet to maintain the temperature of the latter below the recommended maximum of 600° F. The asbestos-cement sheets on which the heating units are assembled are supported on a light structural-steel frame. The graphite rods are assembled into arrays in which the length, number, and spacing of rods are varied to suit the size of the specimen and the density of power dissipation desired. In the present tests the radiator (fig. 13) consisted of 48 rods of 21-inch active length and 3/8-inch diameter at 1-inch spacing. These rods had a drop of approximately $2\frac{1}{2}$ volts per inch of length with a current of 800 amperes flowing. A reflector consisting of 1/4-inch clad aluminum plate was placed behind the rods.

Power Supply

Radiators of this type are used with adjustable-voltage and with constant-voltage power sources. In the present investigation power was supplied from two adjustable-voltage motor-alternator sets, each of 1,000 kilovolt-ampere capacity at 460 volts, three phase. Each motor-alternator supplied one-half the radiator; thus, the 48 rods of the radiator were connected in two 3-phase delta banks with 8 rods in each

phase. Adjustable-voltage power sources are advantageous in that operation can be conducted at any power level within the range of the equipment, and power to the radiator can be varied with time or maintained constant during the heating test.

The limitation on maximum power dissipation per unit frontal area of the radiator, and therefore the limitation on maximum heating rate with the present type of apparatus, appears to be the occurrence of arcs between adjacent rods. When the rods are heated to incandescence, quantities of graphite particles are driven off the surfaces of the rods and these particles form conducting paths through the air between rods. Operation of the radiator during arcing appears undesirable for several reasons: The current to the radiator fluctuates rapidly, radiation from local areas undergoing arcing will be variable, and it is possible that the specimen may be damaged by an arc from the radiator to the specimen. In order to reduce arcing with the present radiator, ceramic barriers were placed between the rods.

Because of the loss of material from the surface of a rod during heating, the rods have a limited useful lifetime. At power levels such as used in the present tests the rods have a life of approximately 2 minutes at operating temperature. This life is sufficient to make 4 to 6 rapid-heating tests. As the graphite rods diminish in size with use, the electrical resistance increases and the power dissipated decreases. This decrease amounts to about 20 percent of the power after 2 minutes use. With an adjustable-voltage power supply, however, the power to the rods can be adjusted to compensate for the changing rod characteristics.

Thermal Shield

The thermal characteristics of the graphite rods require the use of a thermal-radiation shield between the rods and test specimen to control the heat supplied to the specimen. At the start of a heating cycle, the graphite rods require 15 seconds, or longer, to come to operating temperature; after the power to the rods is shut off, the rods require several minutes to cool. The thermal shield is interposed between the heater and specimen before a heating test is started. When the rods reach the desired operating condition, the shield is withdrawn and the specimen is exposed to heat. After the desired temperature or heating time is reached, the shield is again interposed. The thermal shield consisted of a 1-inch-thick sheet of insulating board faced with 1/4-inch-thick asbestos sheet on the heater side. The asbestos sheet was deteriorated rapidly by the intense heat and was periodically replaced.

In the present tests the one-piece thermal shield was manually withdrawn. A two-piece shield, actuated by compressed air, has been developed for use in future tests. In the two-piece shield the two halves of the

shield part on a line parallel to the longitudinal axis of the specimen and move away from each other in order to expose the specimen to the heat symmetrically and more rapidly.

Performance of Radiator

Figure 14 shows the radiator in operation during one of the heating tests. The thermal shield has been withdrawn and the beam is exposed to the radiated heat. This figure clearly shows the large quantities of incandescent carbon particles that are conducive to arcing between rods.

The heating rates achieved with radiant heaters are, of course, affected greatly by the surface condition of the body being heated. Aluminum-alloy sheet in the as-received condition will absorb approximately 20 percent of the incident radiation. In order to increase the absorptivity of the specimens of the present investigation, one coat of flat black lacquer was applied to the surfaces to be heated. Previous tests of surfaces so treated indicated that approximately 90 percent of the incident radiation from the graphite rods is absorbed.

The heating rates produced by the graphite-rod heat radiator in aluminum-alloy sheets coated with black lacquer are shown in figure 15 for various distances between sheet and radiator. Curves for two densities of power input, 180 and 90 kilowatts per square foot of frontal area, are given. The heating rate achieved in the test specimen decreases as the distance from radiating rods to specimen is increased. Because of the presence of the thermal shield, the minimum distance is approximately 2 inches. In the present tests the specimens were approximately 4 inches from the radiator. At the higher of the two input powers shown, a specimen heating rate approaching 100 Btu/ft^2-sec is achieved at a radiator-to-specimen distance of 2 inches. It will be noted that the original objective of a heating rate of 30 Btu/ft^2-sec is possible at distances up to as much as 12 inches and somewhat more.

At the higher input, 180 kilowatts per square foot, shown in figure 15, arc-free operation of the radiator is obtained with rods at 1-inch spacing. The radiator has been operated at power inputs of 230 kilowatts per square foot, which produced heating rates in excess of 100 Btu/ft^2-sec with the specimen approximately 3 inches from the radiator, but some difficulty with arcing was encountered.

APPENDIX B

ELEMENTARY ANALYSIS OF THERMAL STRESSES

The effect of nonuniform temperature distributions on stresses in an idealized multiweb box beam (see fig. 10(a)) is analyzed. The temperature distribution shown in figure 10(b) is an idealization of the distributions measured in the test specimens. A more general analysis of stresses in a stiffened shell structure having a nonuniform temperature distribution is given in reference 1.

The following symbols are defined:

A	cross-sectional area, sq in.
a,m	constants
b_W	depth of section, in.
E	modulus of elasticity, psi
t_W	thickness of web, in.
T	temperature, $^{\circ}F$
y	coordinate axis
α	coefficient of thermal expansion, per $^{\circ}F$
ϵ	normal strain
σ	normal stress, psi

Subscripts:

1	high temperature
2	low temperature
W	web

With the assumption that plane cross sections remain plane, the strain at any point is given by

$$\epsilon = \frac{\sigma}{E} + \alpha T \qquad \text{(B1)}$$

and the stress is

$$\sigma = E(\epsilon - \alpha T) \tag{B2}$$

The linear variation of strain across the section can be written

$$\epsilon = a + my$$

where a and m are constants. Substituting this relation into the expression for stress (eq. (B2)) gives

$$\sigma = E(a + my - \alpha T) \tag{B3}$$

For particular points on the cross section, this equation for normal stress is written with appropriate subscripts. For example,

for high-temperature flange:

$$\sigma_1 = E_1\left(a + my - \alpha_1 T_1\right) \tag{B4a}$$

for low-temperature web adjacent to high-temperature flange:

$$\sigma_{1W} = E_2\left(a + my - \alpha_2 T_2\right) \tag{B4b}$$

for low-temperature flange:

$$\sigma_2 = E_2\left(a - \alpha_2 T_2\right) \tag{B4c}$$

for low-temperature web adjacent to low-temperature flange:

$$\sigma_{2W} = E_2\left(a - \alpha_2 T_2\right) \tag{B4d}$$

The constants a and m can be evaluated with the aid of the equilibrium equations

$$\int \sigma \, dA = 0 \tag{B5}$$

$$\int \sigma y \, dA = 0 \tag{B6}$$

for forces and moments, respectively, on the cross section.

Substitution of equations (B4) into equations (B5) and (B6) gives

$$E_2A_2\left(a - \alpha_2T_2\right) + E_1A_1\left(a + mb_W - \alpha_1T_1\right) + \int_0^{b_W} E_2\left(a + my - \alpha_2T_2\right)t_W\,dy = 0$$

$$E_1A_1b_W\left(a + mb_W - \alpha_1T_1\right) + \int_0^{b_W} E_2\left(a + my - \alpha_2T_2\right)t_Wy\,dy = 0$$

which, after integration, are

$$E_2A_2\left(a - \alpha_2T_2\right) + E_1A_1\left(a + mb_W - \alpha_1T_1\right) + E_2t_W\left(ab_W + \frac{1}{2}mb_W^2 - \alpha_2T_2b_W\right) = 0 \tag{B7}$$

$$E_1A_1b_W\left(a + mb_W - \alpha_1T_1\right) + E_2t_W\left(\frac{1}{2}ab_W^2 + \frac{1}{3}mb_W^3 - \frac{1}{2}\alpha_2T_2b_W^2\right) = 0 \tag{B8}$$

From these expressions the constants are found to be

$$a = \frac{\left(E_1A_1\alpha_1T_1 + E_2A_2\alpha_2T_2 + E_2t_Wb_W\alpha_2T_2\right)\left(E_1A_1 + \frac{E_2t_Wb_W}{3}\right) - \left(E_1A_1\alpha_1T_1 + \frac{E_2t_Wb_W}{2}\alpha_2T_2\right)\left(E_1A_1 + \frac{E_2t_Wb_W}{2}\right)}{\left(E_1A_1 + E_2A_2 + E_2t_Wb_W\right)\left(E_1A_1 + \frac{E_2t_Wb_W}{3}\right) - \left(E_1A_1 + \frac{E_2t_Wb_W}{2}\right)^2}$$

$$mb_W = \frac{\left(E_1A_1\alpha_1T_1 + \frac{E_2t_Wb_W}{2}\alpha_2T_2\right)\left(E_1A_1 + E_2A_2 + E_2t_Wb_W\right) - \left(E_1A_1\alpha_1T_1 + E_2A_2\alpha_2T_2 + E_2t_Wb_W\alpha_2T_2\right)\left(E_1A_1 + \frac{E_2t_Wb_W}{2}\right)}{\left(E_1A_1 + E_2A_2 + E_2t_Wb_W\right)\left(E_1A_1 + \frac{E_2t_Wb_W}{3}\right)\left(E_1A_1 + \frac{E_2t_Wb_W}{2}\right)^2}$$

Substitution of these values of the constants into equation (B4a) gives

$$\sigma_1 = -E_1(\alpha_1 T_1 - \alpha_2 T_2) \frac{1 + 4\dfrac{E_2 A_2}{E_2 t_W b_W}}{1 + 4\dfrac{E_1 A_1}{E_2 t_W b_W} + 4\dfrac{E_2 A_2}{E_2 t_W b_W} + 12\dfrac{(E_1 A_1)(E_2 A_2)}{(E_2 t_W b_W)^2}} \tag{B9}$$

Similarly, equations (B4b) to (B4d) can be evaluated.

The buckling stress in the heated covers of the box beams tested can be calculated by substitution of the following values (corresponding to the temperatures at buckling) into equation (B9):

$T_1 = 580^\circ$ F	$T_2 = 80^\circ$ F
$E_1 = 7.9 \times 10^6$ (ref. 2)	$E_2 = 10.7 \times 10^6$
$\alpha_1 = 14.6 \times 10^{-6}$ (ref. 3)	$\alpha_2 = 12.5 \times 10^{-6}$
$A_1 = 0.49$	$A_2 = 0.49$
	$t_W b_W = 0.64$

The values of A_1 and A_2 were obtained by dividing the total cross-sectional area of the cover by the number of webs. The value of $t_W b_W$ is the area of one web including attachment flanges.

The calculation yields a compressive thermal stress of 20,900 psi in the cover at the average temperature at which buckling was observed in all the beams.

REFERENCES

1. Heldenfels, Richard R.: The Effect of Nonuniform Temperature Distributions on the Stresses and Distortions of Stiffened-Shell Structures. NACA TN 2240, 1950.

2. Roberts, William M., and Heimerl, George J.: Elevated-Temperature Compressive Stress-Strain Data for 24S-T3 Aluminum-Alloy Sheet and Comparisons With Extruded 75S-T6 Aluminum Alloy. NACA TN 1837, 1949.

3. Heimerl, George J., and Inge, John E.: Tensile Properties of 7075-T6 and 2024-T3 Aluminum-Alloy Sheet Heated at Uniform Temperature Rates Under Constant Load. NACA TN 3462, 1955.

TABLE I

TEST DATA AND RESULTS FOR BOX BEAMS SUBJECTED TO RAPID HEATING

	Beam 1	Beam 2	Beam 3	Beam 4
	With ribs		Without ribs	
Heating rate, Btu/ft^2-sec	90	29	77	24
Maximum temperature rate, ^{o}F/sec	224	70	188	59
Heating time to buckling, sec	2.3	8.4	2.8	9.2
Average skin temperature at buckling, ^{o}F	555	590	560	565
Heating time to maximum temperature, sec	4	16	4	12
Maximum skin temperature, ^{o}F	1,040	1,140	800	800

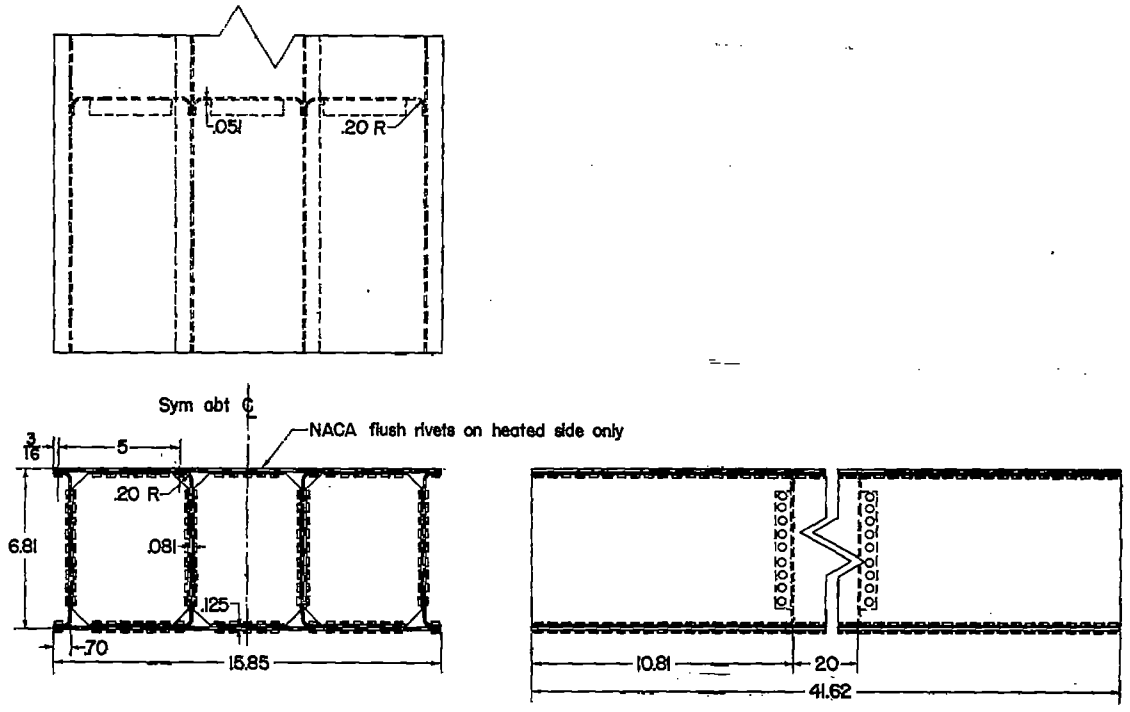

Figure 1.- Multiweb box beams. All dimensions are in inches.

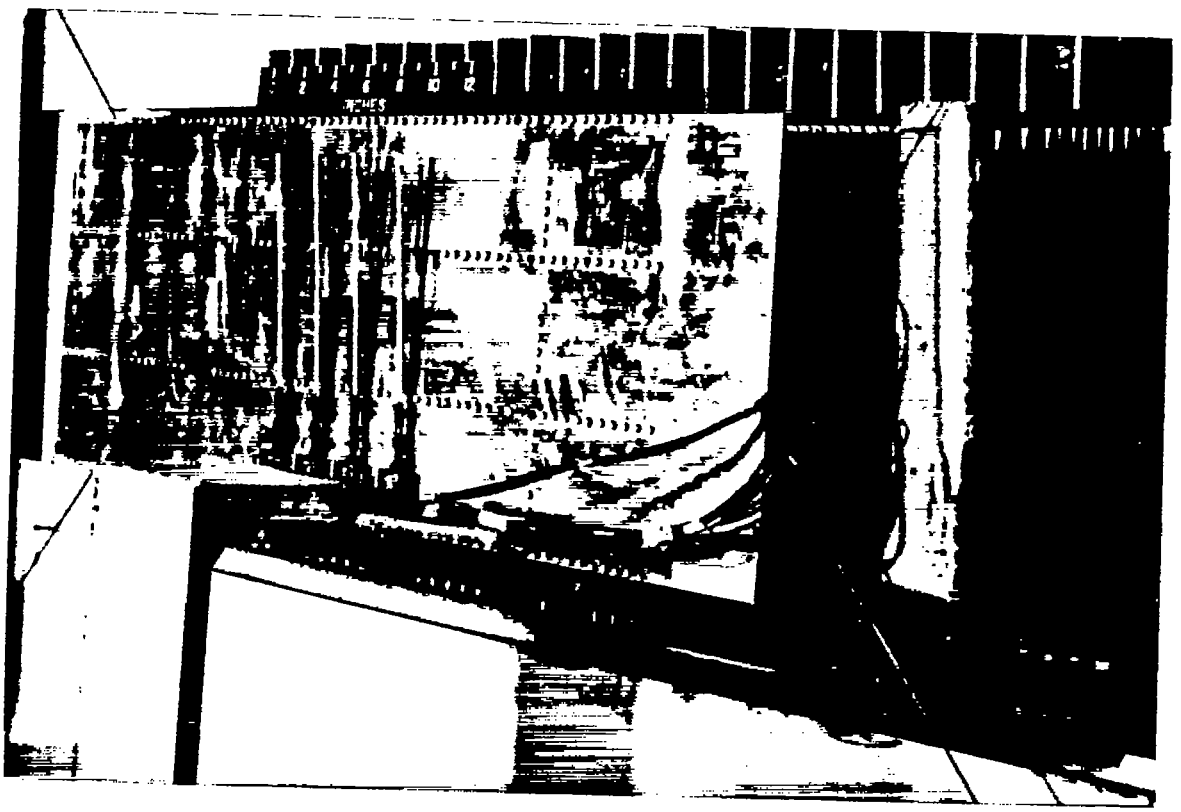

L-84007.1

Figure 2.- Multiweb box beam in front of heat radiator.

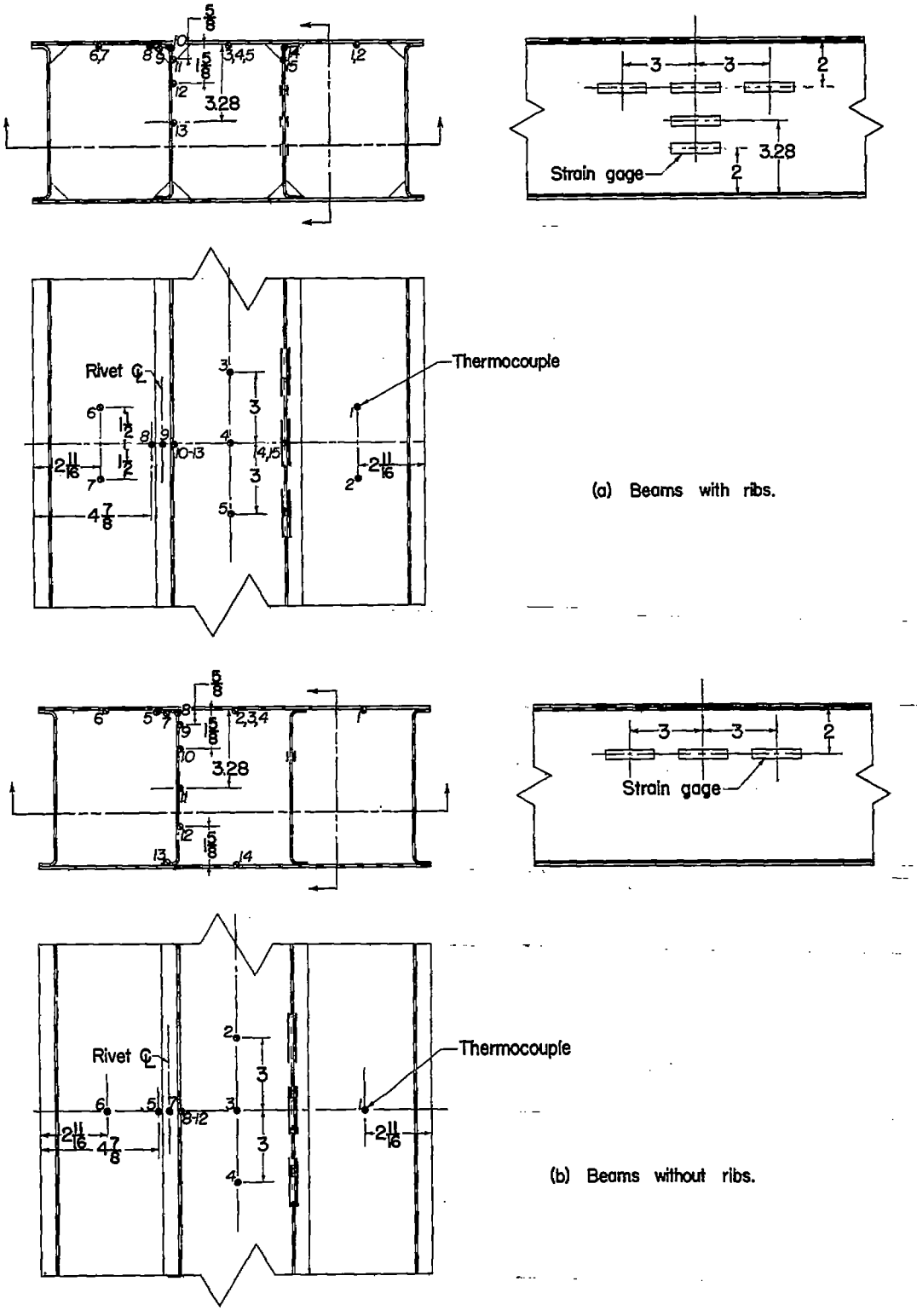

Figure 3.- Instrumentation of box beams.

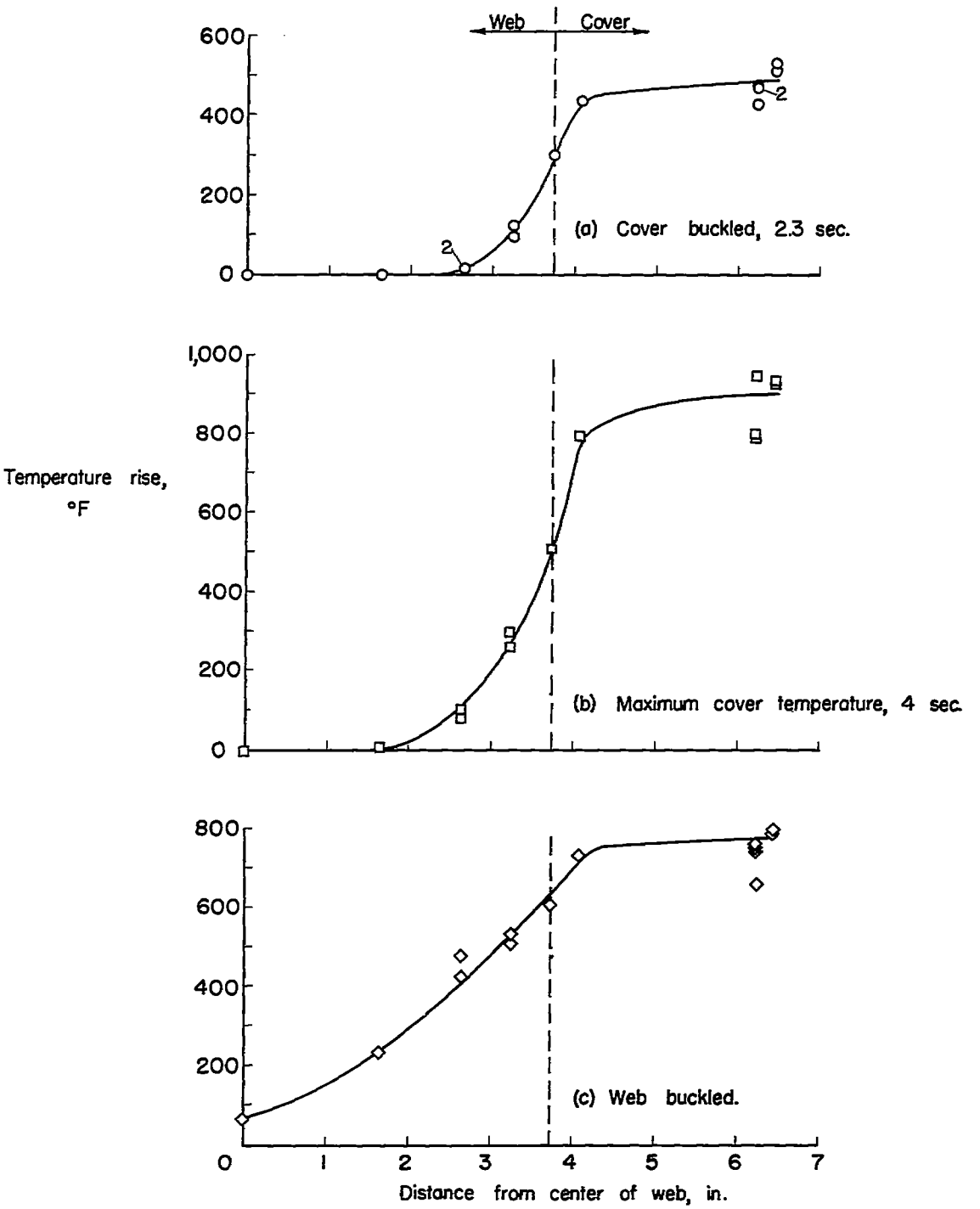

Figure 4.- Temperature distribution in beam 1. Heating rate, 90 Btu/ft^2-sec.

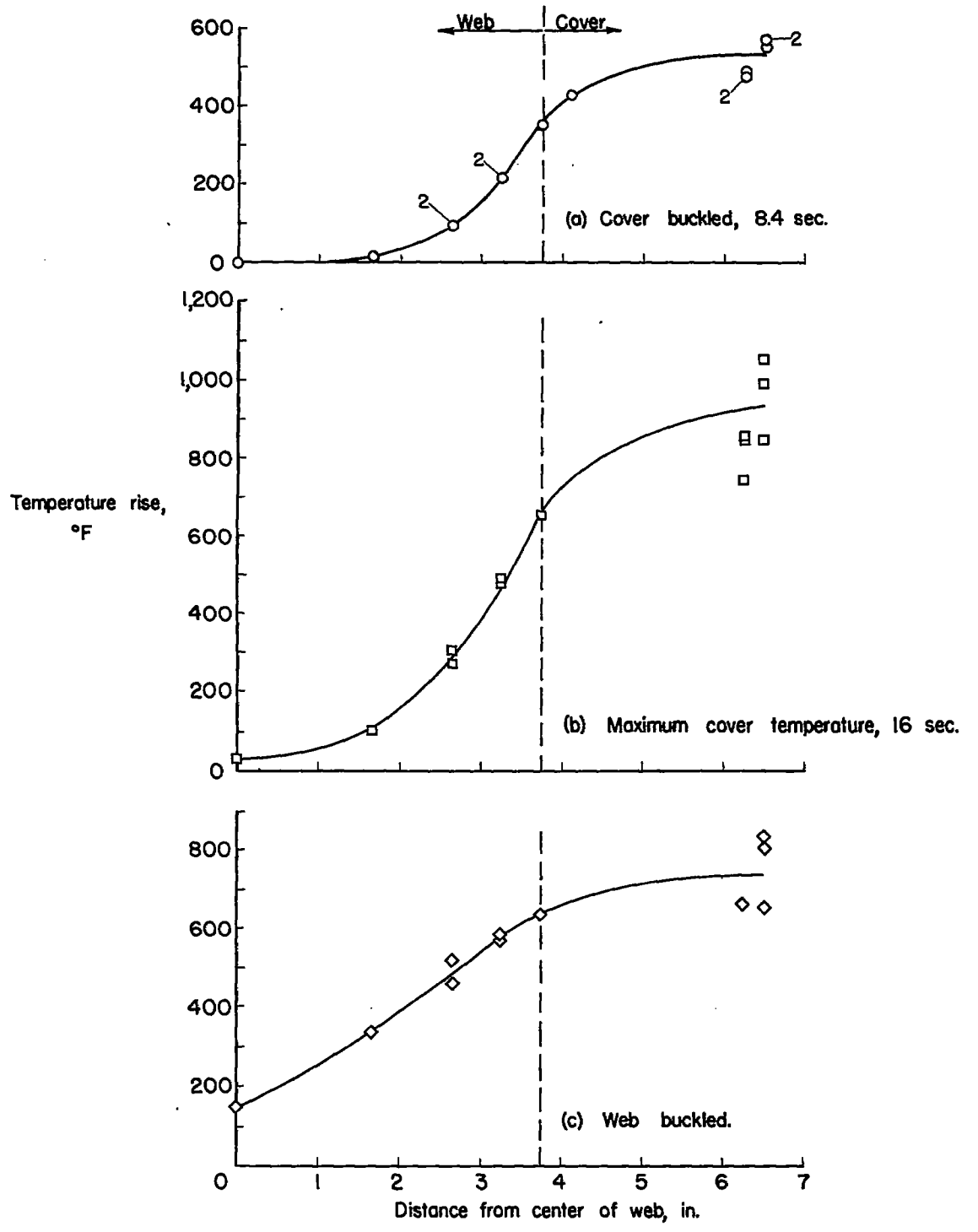

Figure 5.- Temperature distribution in beam 2. Heating rate, 29 Btu/ft^2-sec.

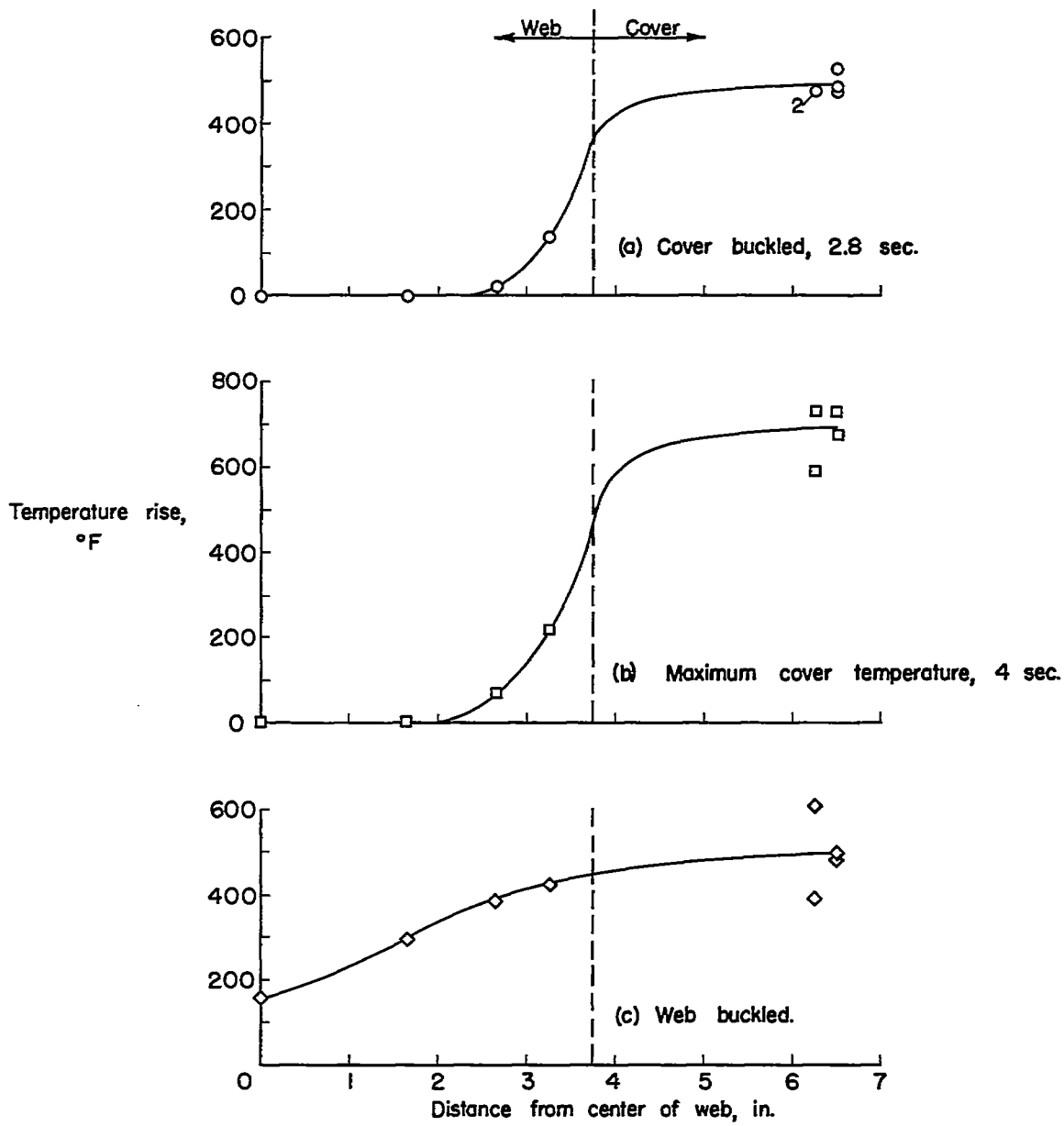

Figure 6.- Temperature distribution in beam 3. Heating rate, 77 Btu/ft^2-sec.

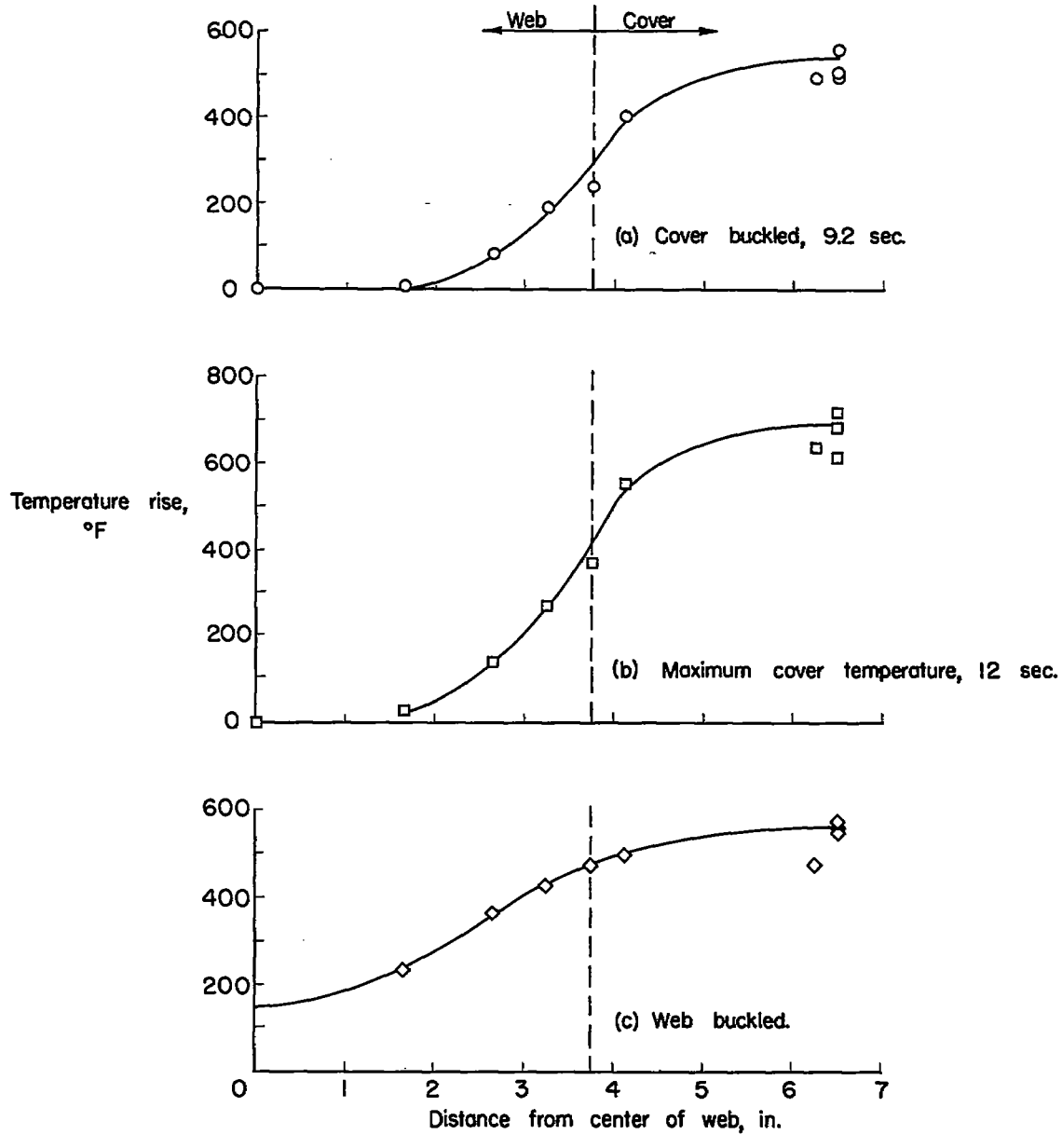

Figure 7.- Temperature distribution in beam 4. Heating rate, 24 Btu/ft^2-sec.

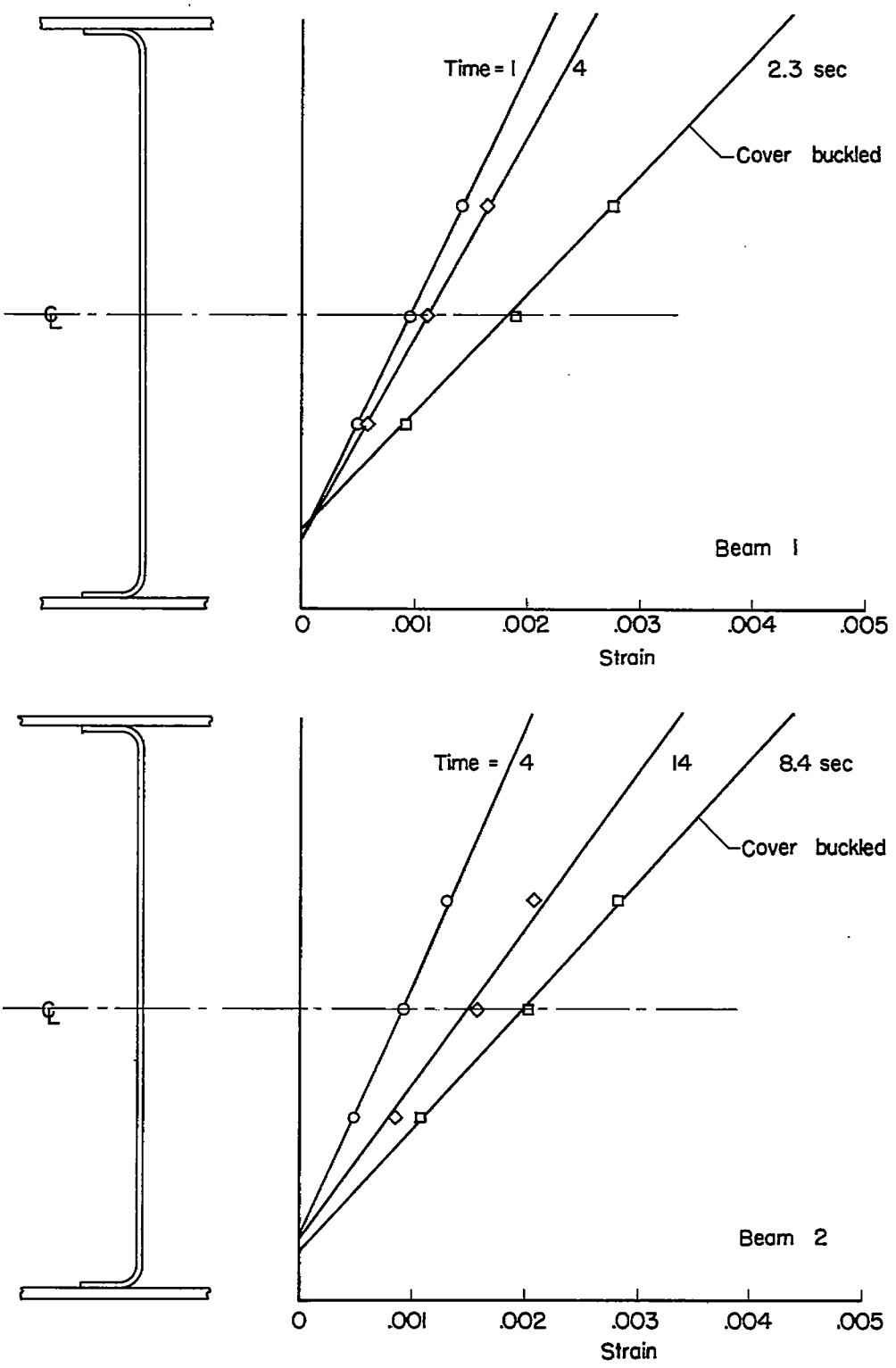

Figure 8.- Measured longitudinal strains in webs during heating.

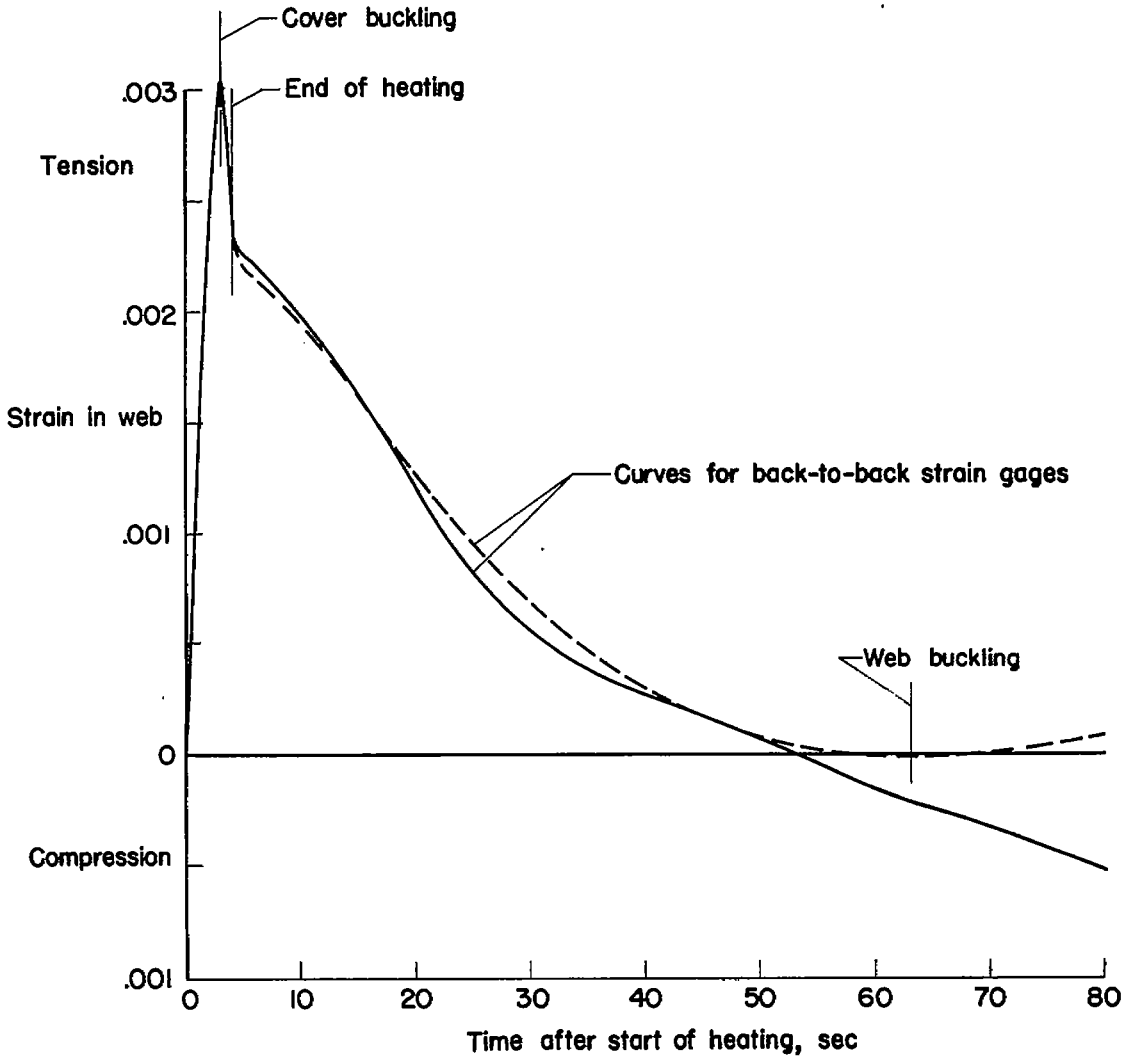

Figure 9.- Time history of strain at center of web. Beam 3.

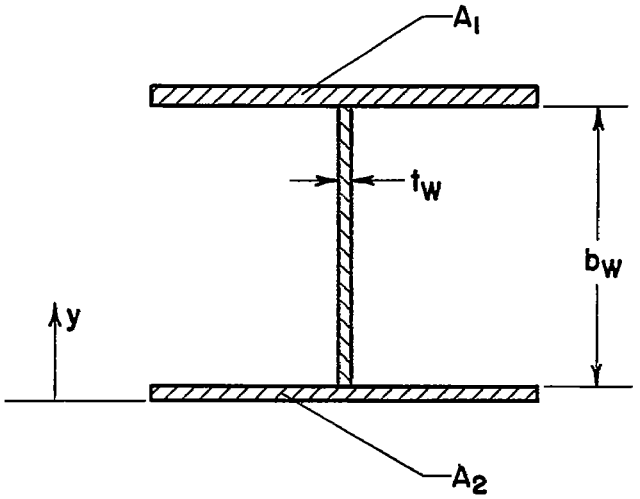

(a) Idealized section.

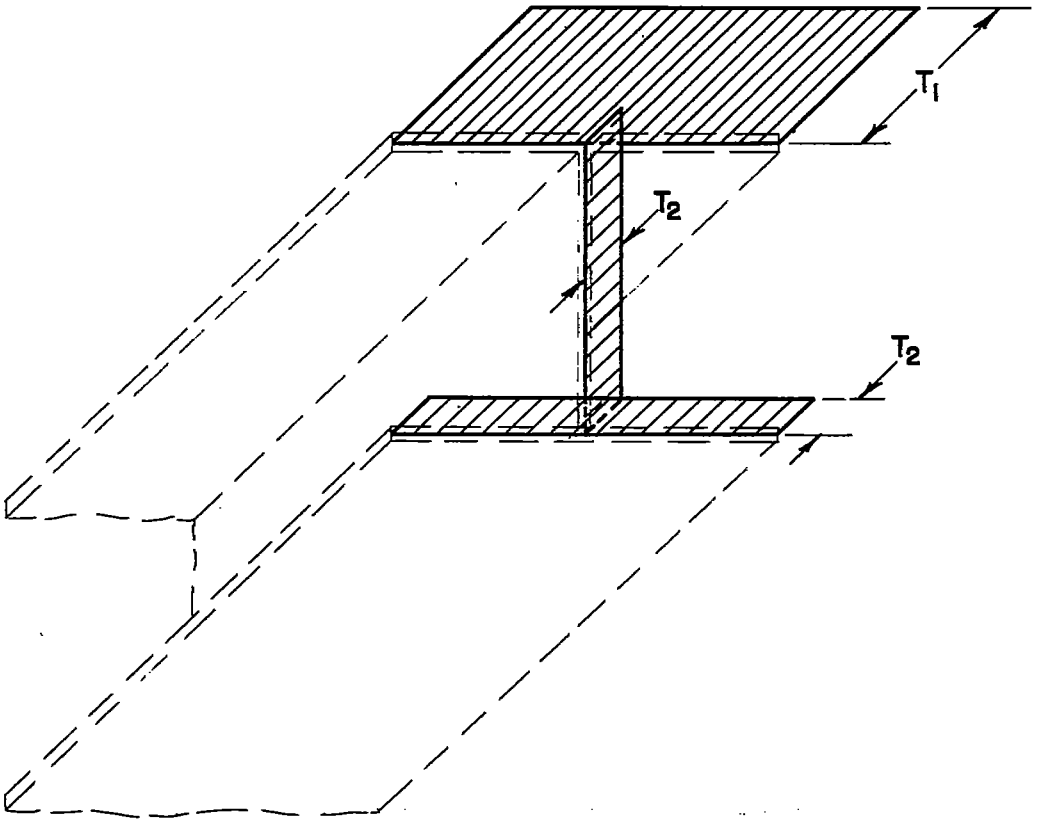

(b) Idealized temperature distribution.

Figure 10.- Model used for thermal-stress analysis.

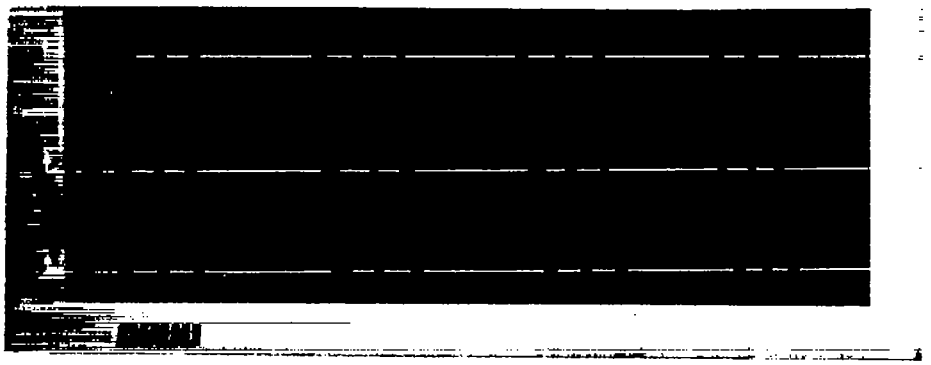

(a) Cover before heating. L-83582.1

(b) Cover after heating. L-83816.1

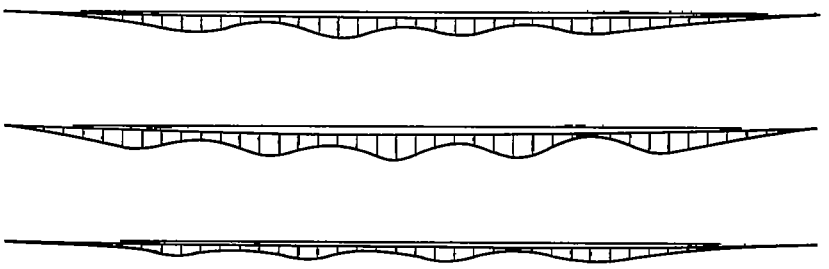

(c) Buckle profiles in cover midway between webs.

Figure 11.- Typical beam deformations after heating.

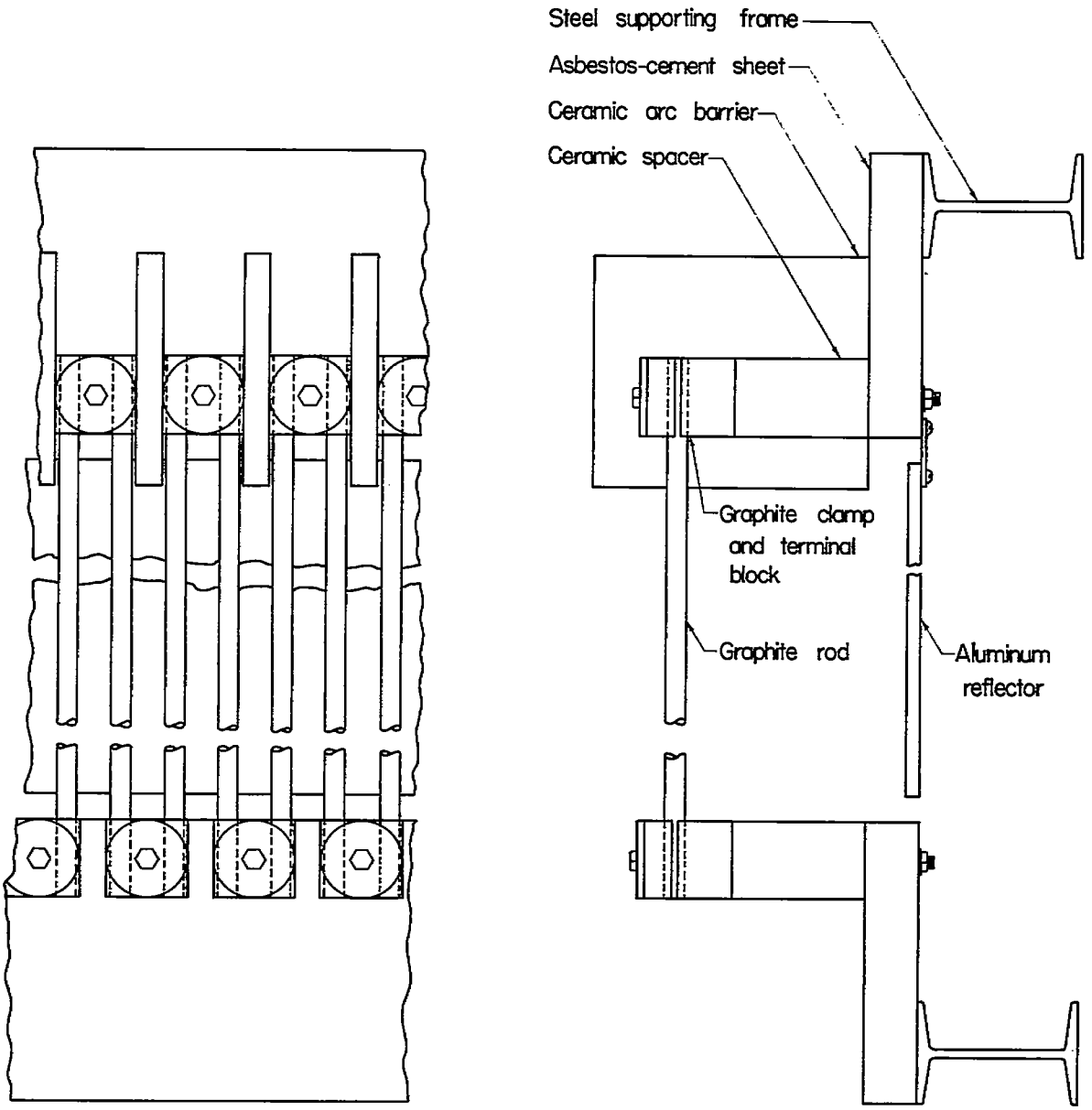

Figure 12.- Construction of graphite-rod heat radiator.

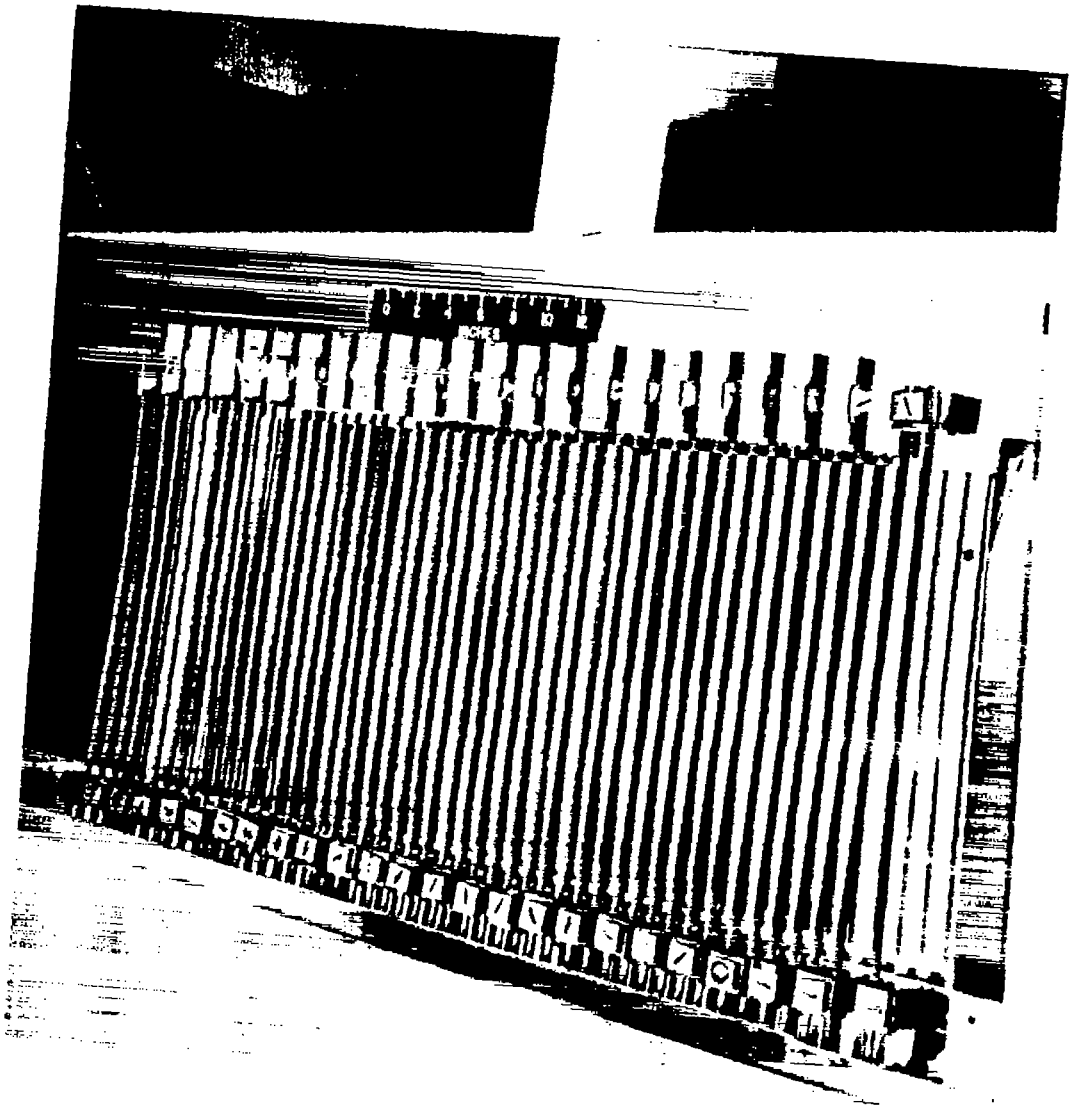

Figure 13.- Transient heating apparatus employing graphite-rod heating elements. L-84008.1

L-84111.1

Figure 14.- Multiweb box beam subjected to rapid heating by radiation from graphite-rod heat radiator.

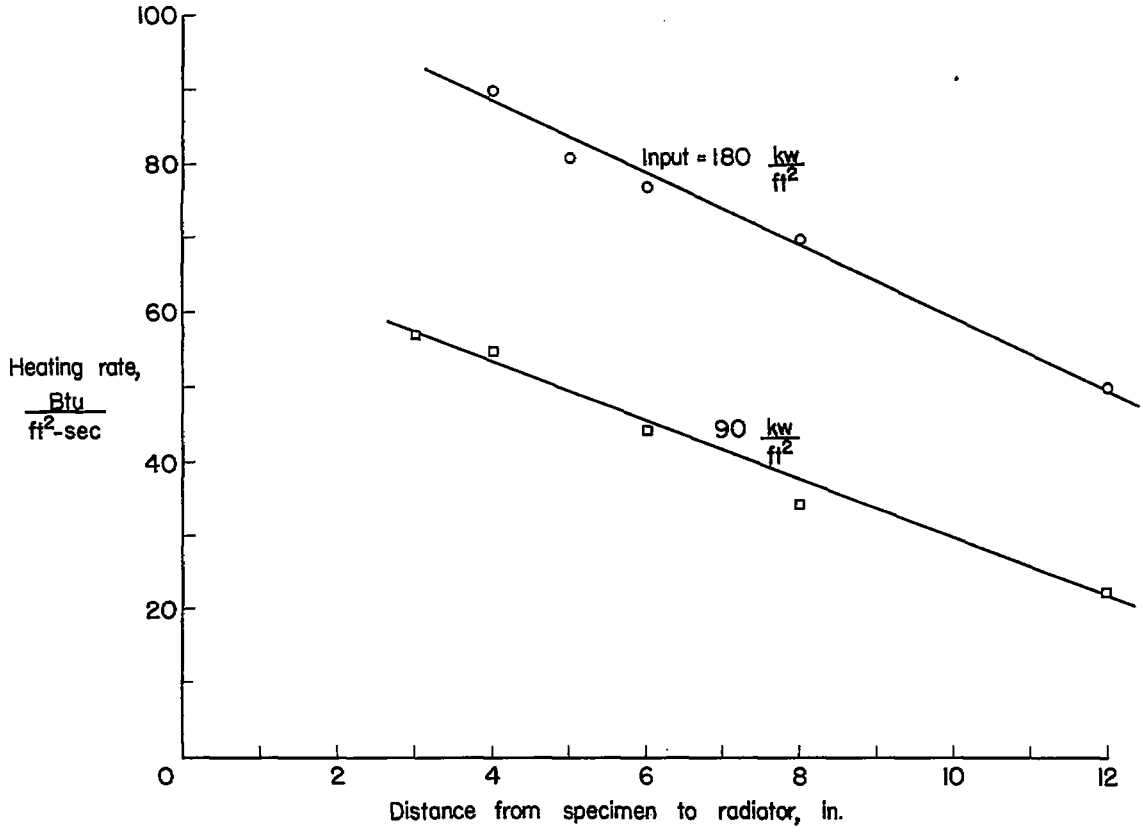

Figure 15.- Heating rates produced by graphite-rod heat radiator. Aluminum-alloy sheet coated with flat black lacquer.